Efficient Hyperpolarised 13C Metabolic Imaging with Rosette Spectroscopic Imaging

R. F. Schulte[1], F. Wiesinger[1], K. M. Fish[2], D. Whitt[2], and I. Hancu[2]

[1]GE Global Research, Munich, Germany, [2]GE Global Research, Niskayuna, NY, United States

Introduction

Metabolic imaging with hyperpolarised $^{13}C_1$-pyruvate [1] requires efficient spectral-spatial sampling schemes in order to acquire as much information from the precious non-recoverable polarisation as possible. One approach is to excite the magnetisation with a small-tip angle and apply efficient readout trajectories during the FID, like for instance EPSI (echo-planar spectroscopic imaging) [2] or spiral CSI [3]. A particularly efficient readout trajectory is rosette [4]. In this work, we show initial *in vivo* results for the application of rosette to metabolic imaging with hyperpolarised $^{13}C_1$-pyruvate.

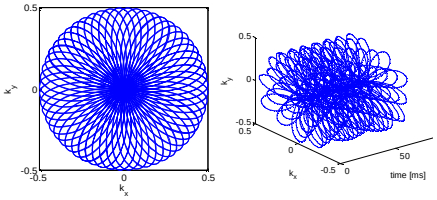

Fig.1: Rosette sampling pattern with two spatial dimensions (k_x, k_y). The spectral encoding capabilities become apparent when k_x and k_y are plotted against the time (right).

Theory and Methods

The rosette trajectory (Fig. 1) consists of an oscillation f_1 and a rotation f_2

$$k(t) = k_{\max} \sin(2\pi f_1 t) e^{i 2\pi f_2 t}.$$

Main feature of rosette sampling is a frequent crossing of the trajectory through the centre of k-space. Acquiring the same locations in k-space multiple times leads to a spectral selectivity which can be utilised to distinguish metabolites with different chemical shifts, in the present case $^{13}C_1$ pyruvate (Pyr) and its metabolic derivatives $^{13}C_1$ alanine (Ala) and $^{13}C_1$ lactate (Lac). Important to consider is the complex nature of under-sampling artefacts. Only the centre of k-space is densely sampled; the trajectory returns only rarely to similar high spatial frequencies. Hence, under-sampling of high spatial frequencies occurs, folding signal back both spectrally and spatially. This aliasing appears seemingly incoherent (i.e., noise-like).

Female Sprague-Dawley rats with a weight of 250-300g were purchased from Charles River Laboratories with catheters implanted in the left common carotid artery, with the tip of the catheters pointing towards the aorta. They were anaesthetised i.p. with Ketamine/Diazepam (75/5 mg/kg) and injected with 80mM hyperpolarised, $^{13}C_1$ pyruvate, at a dose of 5ml/kg. Liquid state polarisation levels at the time of injection were 10% (rat a) and 6% (rat b). Acquisition of the 13C rosette sequence started 12s (a) and 22s (b) after injection.

The same axial slice (FOV=100mm; slice thickness=10mm) was acquired both with a ^{1}H GRE sequence (TEs=10ms,11ms,13ms; res=160×100) and the ^{13}C rosette sequence. The parameters for the rosette sequence were f_1=221Hz, f_2=71Hz, 4 interleaves, t_{acq}=65ms, flip angle=40°, which led to g_{max}=20.8mT/m, s_{max}=31.8T/m/s and a resolution after gridding of 32×32. Data were acquired on a 1.5T GE Signa HDx scanner (software release 14M5; GE Healthcare, Milwaukee, USA).

For the reconstruction, the data was down-sampled from a bandwidth of BW=62.5 kHz and 4096 acquisitions points to a quarter of BW and points, respectively. The density compensation function was calculated with Voronoi triangulation, and the data was filtered in k-space and time with a Gaussian filter. The reconstruction included a shift to the actual chemical shift frequency by multiplying the according phase kernel to the data, a fast gridding algorithm [6] to interpolate the data to a Cartesian grid, zero-filling to 64×64 and fast Fourier transformation. The results were compared to MFI (multi-frequency interpolation) reconstruction [7] to compensate for B_0 inhomogeneities. B_0 maps were obtained both with separate measurements on proton frequency and auto-calibration on the pyruvate frequency. For comparison, rosette data was acquired on proton frequency with the similar acquisition parameters and reconstructed accordingly. All post-processing algorithms were implemented in Matlab R2007b (Mathworks, Natick, USA).

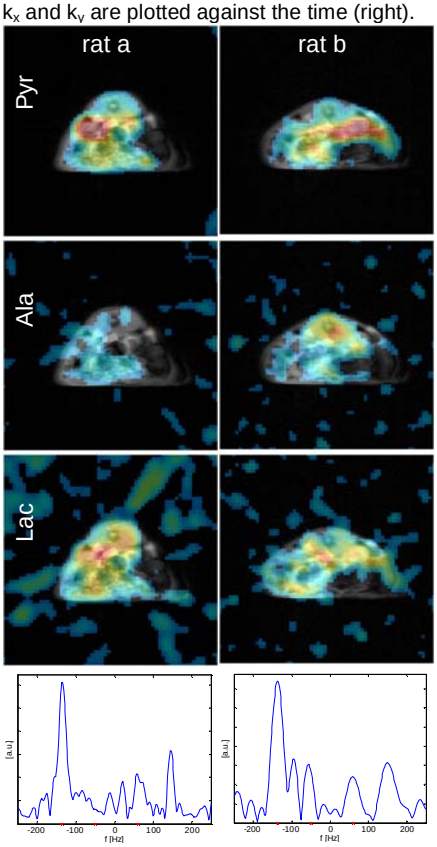

Fig. 2: Pyr, Ala, Lac images (f=-137,-50 60Hz) and spectrum (from top to bottom) for rat a (left) and b (right). The colour-map was exaggerated by a factor of 3 (a) and 1.5 (b) for both Ala and Lac.

Results and Discussion

It is possible to detect and distinguish Pyr, Ala and Lac *in vivo* (Fig. 2). While Pyr always shows a good SNR, Ala and Lac are closer to the detection limit. In case of Ala, the detection was only possible in rat b, where the time from injection to acquisition was longer, and hence the conversion from Pyr was larger. The signal is particularly strong around the kidney, but disappears near the catheter due to field inhomogeneities. There was no big difference between normal gridding and MFI reconstruction in terms of signal cancellation and strength. Reasons for this include fairly large voxel sizes as compared to the variations in B_0 and also a smaller impact of B_0 inhomogeneities both because of the low field strength (1.5T) and the lower gyro-magnetic ratio (γ) of ^{13}C (a quarter as compared to ^{1}H). The impact of a higher γ is visible in ^{1}H rosette data in Fig. 3, which could be improved by auto-calibrated MFI reconstruction [8].

Conclusion

Rosette is a viable sequence for an efficient spectral and spatial encoding and has the potential to acquire multiple time steps in the metabolism. Future work will concentrate on 3T with its better spectral separation and on acquiring more steps in the metabolism.

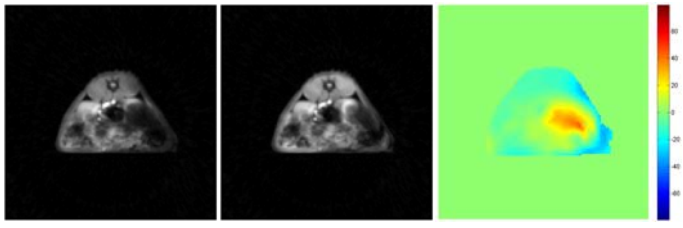

Fig. 3: Proton rosette of rat a (32 interleaves; 128×128) reconstructed with gridding (left) and MFI (middle). The auto-calibrated B_0 map (in Hz) as used for MFI is shown on the right.

References

[1] Golman K, *et al*. PNAS USA 2003;100:10435.
[2] Cunningham CH, *et al*. MRM 2005;54:1286.
[3] Mayer D, *et al*. MRM 2006;56:932.
[4] Noll DC. IEEE TM Imag 1997;16:372.
[5] Derby K, *et al.* JMR 1990;86:645.
[6] Beatty PJ, *et al*. IEEE TM Imag 2005;24:799.
[7] Man LC, *et al.* MRM 1997;37:785.
[8] Wiesinger F. *et al*. ISMRM 2008;790.